A Compact Rayleigh and Rician Fading Simulator Based on Random Walk Processes

Amirhossein Alimohammad, Saeed F. Fard, Bruce F. Cockburn, Christian Schlegel
Department of Electrical and Computer Engineering, University of Alberta, Edmonton, Canada
Email:{amir,saeed,cockburn,schlegel}@ece.ualberta.ca

***Abstract*— This article describes a significantly improved sum-of-sinusoids-based model for the accurate simulation of time-correlated Rayleigh and Rician fading channels. The proposed model utilizes random walk processes instead of random variables for some of the sinusoid parameters to more accurately reproduce the behavior of wireless radio propagation. Every fading block generated using our model has accurate statistical properties on its own and hence, unlike previously proposed models, there is no need for time-consuming ensemble-averaging over multiple blocks. Using numerical simulation it is shown that the important statistical properties of the generated fading samples have excellent agreement with the theoretical reference functions. A fixed-point hardware implementation of the corresponding Rayleigh and Rician fading channel simulator on a field-programmable gate array (FPGA) is presented. By efficiently scheduling the operations, the reconfigurable fading channel simulator is compact enough that it can be efficiently used to simulate multipath scenarios and multiple-antenna systems (e.g., a 4×4 MIMO channel) using a single FPGA.**

List of Acronyms— Wide-sense stationary (WSS), power spectral density (PSD), sum-of-sinusoids (SOS), autocorrelation function (ACF), cross-correlation function (CCF), field-programmable gate array (FPGA), multiple parameter set (MPS), random walk process (RWP), line-of-sight (LOS), probability density function (PDF), cumulative distribution function (CDF), level crossing rate (LCR), average fade duration (AFD), pseudo-random number generator (PNG), read-only memory (ROM), Block RAM (BRAM).

I. Introduction

The successful design and testing of emerging wireless technologies requires the accurate simulation of radio propagation environments. The simulation model must faithfully reproduce the statistical behavior of the wireless channel to ensure accurate evaluation of proposed systems under realistic fading conditions. The temporal behaviour of a fading channel is commonly modeled as a complex Gaussian WSS uncorrelated scattering process with complex envelope $c(t) = c_i(t) + jc_q(t)$ [1]. In this model, the real and imaginary parts of the complex Gaussian process $c(t)$, $c_i(t)$ and $c_q(t)$, are independent, zero-mean Gaussian with equal variance [2]. Thus the envelope $|c(t)| = \sqrt{c_i(t)^2 + c_q(t)^2}$ follows the Rayleigh distribution $f_{|C|}(c) = \frac{c}{\sigma^2} \exp\big[-c^2/(2\sigma^2)\big]$, where σ^2 is the time-averaged power of the fading process at the receiver. Under the common assumption of a two-dimensional isotropic scattering environment with an omnidirectional receiving antenna [3], the ideal reference correlation properties of the fading samples can be summarized as follows:

$$
\begin{aligned}
\mathrm{R}_{c_i,c_i}(\tau) &= \mathrm{R}_{c_q,c_q}(\tau) = \mathrm{E}\big[c_q(t)c_q(t+\tau)\big] = \mathcal{J}_0(2\pi f_D \tau) \\
\mathrm{R}_{c_i,c_q}(\tau) &= \mathrm{R}_{c_q,c_i}(\tau) = 0 \\
\mathrm{R}_{c,c}(\tau) &= \mathrm{E}[c(t)c^*(t+\tau)] = 2\,\mathcal{J}_0(2\pi f_D \tau)
\end{aligned}
$$

where f_D is the maximum Doppler frequency, τ is the time lag, $\mathcal{J}_0(\cdot)$ is the zeroth-order Bessel function of the first kind, $\mathrm{R}_{c_i,c_i}(\tau)$ and $\mathrm{R}_{c_q,c_q}(\tau)$ are the autocorrelation functions of the $c_i(t)$ and $c_q(t)$ components of $c(t)$, respectively, $\mathrm{R}_{c_i,c_q}(\tau)$ is the cross-correlation between the components, and $\mathrm{R}_{c,c}(\tau)$ is the autocorrelation of the complex envelope of $c(t)$.

To produce a fading process with the above statistical properties, one approach is to pass white Gaussian variates through a linear filter that has a transfer function equal to the square root of the Doppler PSD of the fading process [4]. This approach, called filter-based henceforth, can be customized to accurately provide the required statistical properties of fading channels [5]. Due to the accuracy of this model, many commercially-available fading channel simulators [**?**], [6]–[9] employ the filter-based technique. However, this approach has high computational complexity [10], relative inflexibility compared to other models, and constraints on the maximum sampling rate posed by the required filter stages.

An alternative implementation strategy is based on the SOS channel model [3], [11]. In this approach, the fading process is modeled by superimposing sinusoidal waveforms with amplitudes, frequencies and phases that are selected appropriately to generate the required statistical properties. Compared to the filter-based method, the SOS model is more flexible, especially for accommodating different Doppler frequencies and symbol rates. In addition, it has been shown that it is possible to achieve accurate statistical properties with a relatively small number (e.g., $N \leq 12$) of sinusoids [12]–[14]. Thus, in contrast to the filter-based method, SOS channel simulators require much less computation and are good potential candidates for hardware implementation.

Several commercial fading channel emulators are available that reproduce the behaviour of radio propagation environments in the laboratory. They are generally stand-alone units that provide the fading signal in the form of analog or digital

TABLE I

SOME COMMERCIALLY AVAILABLE FADING SIMULATORS

Model [a]	A	B	C	D	E
Number of channels	2	2	2	2	6
Number of paths	12	24	48	12	6
Max. Doppler (*Hz*)	800	2000	2400	1600	340
Doppler resolution (*Km/h*)	0.1	0.1	0.1	0.1	0.5
Max. delay (*ms*)	0.2	2	10	1.6	0.04
Time resolution (*ns*)	0.5	0.1	1	50	40

[a](A) Japan Radio Co. NJZ-1600B [9], (B) Spirent Communications SR5500 [8], (C) Agilent Technologies Inc. N5115A [6], (D) Rohde & Schwarz ABFS [16], and (E) Ascom Ltd. SIMSTAR [7].

samples. They require relatively complex hardware consisting of several circuit cards with multiple processors. For example, the NoiseCom MP-2500 Multipath Fading Emulator [15] consists of 11 circuit boards, not including the RF circuitry, the cooling fans, or the external computer interface that is required to set up the various parameters of a frequency-selective fading channel with up to 12 paths. Unfortunately these systems are rather bulky and costly. Characteristics of some of the available fading channel emulators in the market are listed in Table I. The units are available at prices ranging between \$24,000 to \$500,000.

A more flexible and cost-effective approach is to implement the entire fading simulator on a FPGA. In the Monte Carlo performance verification of communication systems, it is desirable to include all of the computationally-critical algorithms in the simulation chain on the same FPGA. Recent advances in FPGA technology now permit the integration of a high-quality fading channel simulator along with a noise generator [17] and signal processing blocks for rapid prototype design and verification.

Even though SOS-based models have been widely-used as the basis for both Rayleigh [18], [19] and Rician [20]–[22] fading channel simulators, unfortunately, many of the proposed SOS-based fading channel models have at least one undesirable statistical property that deviates from the reference properties [23], [24]. For example, the models in [18], [25] have different ACFs for the in-phase and quadrature components of the fading process [26] and the model in [20] is not WSS [22]. A detailed comparison of various SOS-based models can be found in [24] and [27].

In this article we present an improved SOS-based model upon the model proposed by Zheng and Xiao [13], which requires only a small number of sinusoids to accurately reproduce the statistical properties of wireless radio propagation. However, unlike the model in [13] and any other previously proposed SOS-based fading model, in our new model at least one of the parameters of the sinusoids is not a constant or a randomly-generated variable but is instead a random process. Through numerical simulations we will show that the statistical properties of every generated fading block (also called a simulation trial) using our new model accurately match the reference functions. To the best of our knowledge, the proposed stochastic SOS-based model is the first model that generates fading blocks where each block on its own has accurate statistical properties. Therefore, there is no need for time-consuming ensemble averaging over multiple blocks to achieve statistically accurate fading processes. In addition, our proposed fading channel simulator is readily scalable and can be efficiently mapped onto the regular architecture of the FPGA with acceptable computational complexity. Our implementation scheme utilizes an efficient operation schedule, which leads to a significantly smaller simulator than the previous simulators. The proposed fading channel simulator is compact enough to allow an entire 4×4 MIMO channel simulator to fit onto a single FPGA.

The rest of this article is organized as follows. Section II reviews the theory of SOS-based fading simulators. Our new model for simulating Rayleigh and Rician fading channels is presented in Section III. We implemented the Rayleigh fading channel emulator on a variety of FPGA devices and experimentally verified the statistical properties of the generated fading process. Our implementations of a discrete-time Rayleigh fading channel simulator on different FPGAs, and also in 90-nm CMOS technology, are presented in Section IV. Finally, Section V makes some concluding remarks.

II. Related Work on SOS-Based Rayleigh Fading Channel Models

The motivation behind SOS-based fading channel simulators is that when a sinusoidal carrier is transmitted and subjected to multipath fading, the received carrier can be modeled as a superposition of multiple possibly Doppler shifted copies of the transmitted carrier received from different paths. Since the time-varying nature and orientation of obstacles in the wireless channel are not known in advance, the orthogonal components of the received composite complex waveform can be considered to be independent stochastic processes with identical statistics.

Since the introduction of SOS-based fading channel models [1], [28], various fading channel simulators have been proposed [3], [11]–[13], [21], [23], [26], [29]–[32]. Clarke proposed a useful mathematical model for the complex channel gain, valid under the narrow-band flat fading assumption [11]. Clarke showed that the complex channel gain $c(t)$ at time t can be expressed as

$$c(t) = \sqrt{\frac{2}{N}} \sum_{n=1}^{N} \exp\left(j(2\pi f_D t \cos(\alpha_n) + \phi_n)\right) \tag{1}$$

where α_n and ϕ_n are the angle of arrival and the initial phase, respectively, associated with the n-th sinusoid, and N is the total number of sinusoids [11]. In Clarke's model α_n and ϕ_n are mutually independent *random variables* that are uniformly distributed over $[-\pi, \pi)$. When N becomes large, the Central Limit Theorem [33] implies that $\Re\{c(t)\}$ and $\Im\{c(t)\}$ (the real and imaginary components, respectively) are zero-mean, Gaussian and statistically independent. Due to the accurate statistical properties of Clarke's model, it has been used widely as a reference theoretical model for simulating fading channels.

For an efficient implementation of a fading channel simulator using a finite and preferably a small number of sinusoids, various SOS-based models based on Clarke's scheme have been proposed. However, many of the proposed models do not generate statistically accurate fading samples and have fundamental drawbacks. For example, the well-known Jakes fading channel simulator requires a moderate number of sinusoids and it has been studied and used for decades [3]. However, it has been shown (see for example [23], [25]) that Jakes' model is not WSS and that the higher-order statistics of this model do not match those of Clarke's reference model. Several improvements have subsequently been proposed in the literature to enhance the higher-order statistics and make the SOS model WSS.

SOS simulators can be classified either as "deterministic" or "stochastic" [14]. In deterministic SOS simulators, all the waveform parameters (i.e., amplitude, Doppler frequency and phase) are held fixed for the duration of the simulation, and hence the properties of the generated fading process are deterministic. Deterministic SOS-based models has two main drawbacks: (i) in general they require a relatively large number N of sinusoids (e.g., > 32) to achieve accurate statistical properties [34]; (ii) the parameters of the sinusoids are usually deterministic and fixed throughout the simulation. Hence, such models cannot be used to model a fading channel with changing parameters, as would be required to reproduce the statistical properties of time-varying propagation channels.

On the other hand, in the stochastic models at least one of the waveform parameters is a random variable [12]. These models are based on the MPS simulation method [35]. In this approach, a simulation trial is divided into several frames and a new set of random sinusoid parameters (such as random Doppler frequencies and phases) are generated at the start of each frame. For example, to generate 10^7 in-phase and quadrature components, we can divide the trial into 10^3 frames of length 10^4 samples each. In this case, the statistical properties of the generated process change for each simulation trial. It has been shown that with the MPS method, the performance of Monte Carlo simulations is considerably improved [14]. Also, stochastic models require a smaller number of sinusoids compared to deterministic models to achieve similar accuracy.

One widely-referenced stochastic SOS-based model was proposed by Zheng and Xiao [13]. It was shown that this model requires a relatively small number of sinusoids ($8 \leq N \leq 12$) to converge to the desired statistical properties. In the model from [13] (henceforth called *Model I*), the in-phase and quadrature components of the complex envelope of the fading signal can be written in discrete time as follows:

Model I:

$$c_i[m] = \sqrt{\frac{2}{N}} \sum_{n=1}^{N} \cos\left(2\pi f_D T_s m \cos\alpha_n + \varphi_n\right)$$

$$c_q[m] = \sqrt{\frac{2}{N}} \sum_{n=1}^{N} \cos\left(2\pi f_D T_s m \sin\alpha_n + \psi_n\right)$$

and the angle of arrival of the n-th sinusoid is

$$\alpha_n = \frac{2\pi n - \pi + \theta}{4N}, \qquad n = 1, \cdots, N$$

where m is the discrete time index, T_s is the symbol period, $f_D T_s$ is the normalized maximum Doppler frequency, and θ, φ_n and ψ_n are mutually independent *random variables*, uniformly distributed over $[-\pi, \pi)$.

Another stochastic SOS-based fading channel model that has half the computational complexity of *Model I* was proposed by Wu [32]. In this simplified model (henceforth called *Model II*), the in-phase and quadrature components of the complex envelope of the fading signal can be written in discrete time as follows:

Model II:

$$c_i[m] = \sqrt{\frac{1}{N}} \sum_{n=1}^{N} H[n,1] \cos\left(2\pi f_D T_s \cos(\alpha_n) + \phi_n\right)$$

$$c_q[m] = \sqrt{\frac{1}{N}} \sum_{n=1}^{N} H[n,2] \cos\left(2\pi f_D T_s \cos(\alpha_n) + \phi_n\right)$$

and the angle of arrival of the n-th sinusoid is

$$\alpha_n = \frac{2\pi(n+1)}{4N}, \qquad n = 1, \cdots, N.$$

Here the ϕ_n are independent random phases, each of which is uniformly distributed in $[0, 2\pi]$. H denotes an $N \times N$ Walsh-Hadamard matrix whose columns are orthogonal, and $H[i,j]$ denotes the (i,j)-th element of matrix H. Wu utilized these orthogonal weighting functions to guarantee the correlation independence between the in-phase and quadrature components of the fading process.

The key limitation of *Models I* and *II* (and the other stochastic SOS-based models in general) is that their statistical properties converge to the desired properties only over a relatively large number of simulation trials (e.g., 30 simulation trials [36]). The need for averaging over many simulation trials (also called ensemble averaging) implies significantly more computation. Fig. 1 shows that the ACF of the generated fading samples, when averaged over multiple simulation blocks (in this example 10 blocks), can converge to the reference ACF. While *Model I* has a more accurate ACF, the CCF of the generated fading samples using *Model II* approaches the theoretical reference properties more closely, as shown in Fig. 2.

Unfortunately, for the class of stochastic models, such as *Models I* and *II*, the statistical properties of a single simulation trial (i.e., when averaging over time), no matter how many samples are generated in a fading block, do not in general converge to the reference properties. Fig. 3 shows this limitation with a plot of the ACF of the fading process generated using *Models I* and *II* for only one block containing 2×10^6 samples. Clearly the ACF of the fading samples generated using *Model II* deviates significantly from the reference ACF of the Rayleigh fading channel, when measured over only one block. Also, the ACF of the *Model I* deviates from the reference function, especially at the larger

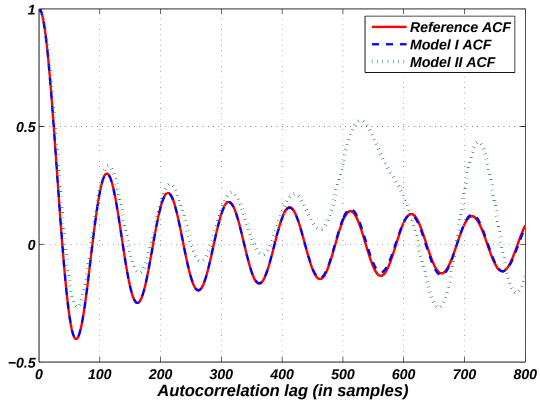

Fig. 1. ACF averaged over 10 blocks containing 10^5 generated fading samples each using *Models I* and *II* with $f_D T_s = 0.01$ and $N = 8$.

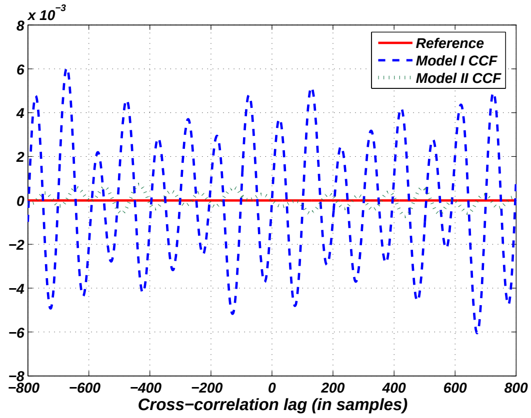

Fig. 2. CCF averaged over 10 blocks containing 10^5 generated fading samples each using *Models I* and *II* with $f_D T_s = 0.01$ and $N = 8$.

lags. Fig. 4 also shows that the CCF between the quadrature components of the fading process over one block is not greatly improved as when the statistics are averaged over many blocks, as shown in Fig. 2.

Ensemble averaging is not only a computationally-expensive process, it also creates unwanted discontinuities in the temporal behavior at the frame boundaries. As a consequence, the testing of a communication system must be interrupted and re-initialized with a new set of random parameters at the start of each frame to ensure accurate modeling of the channel. What is more, the channel estimation or carrier recovery at the receiver must be re-acquired after each draw of random parameters. However, stopping and restarting the communication system and channel simulator in this way might not be convenient in many practical scenarios. Therefore, *Models I* and *II* are not suitable for the real-time emulation of a Rayleigh fading channel with accurate time-averaged statistical properties.

For an efficient implementation of a Rayleigh fading channel simulator, it is crucial to find a SOS model that requires a

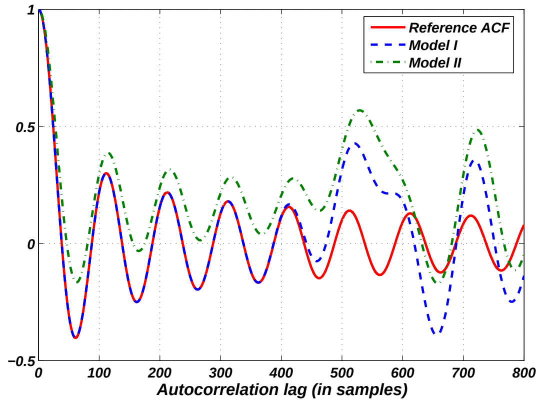

Fig. 3. ACF for one block containing 2×10^6 fading samples using *Models I* and *II* with $f_D T_s = 0.01$ and $N = 8$.

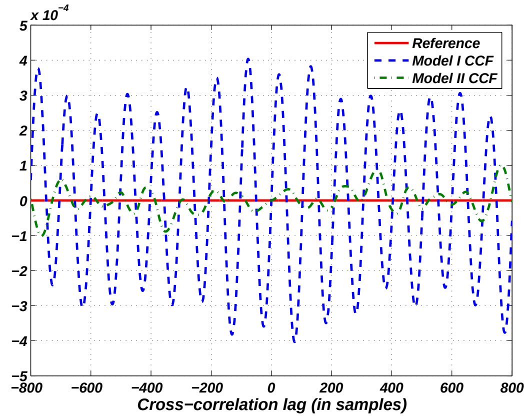

Fig. 4. CCF for one block containing 2×10^6 fading samples using *Models I* and *II* with $f_D T_s = 0.01$ and $N = 8$.

relatively small number of sinusoids to reproduce the desired statistical properties of the fading channel. Also if the channel simulator were to be ergodic, then each simulation trial would produce the same statistics. Hence no ensemble averaging would be required and this would significantly reduce the overall simulation time without creating discontinuities in the temporal behavior [24]. To accurately reproduce the behaviour of radio propagation channels, Zajić and Stüber [36] proposed a deterministic model that is ergodic. However, the autocorrelation of the in-phase and quadrature components of their model does not accurately match the theoretical properties. They also proposed a statistical model to overcome this shortcoming of their deterministic model. Unfortunately, the resulting modified model is no longer ergodic. In the next section we propose a new fading channel model that accurately reproduces the reference statistical properties of a fading process for every generated fading block.

III. New SOS-Based Fading Channel Model

We propose a significantly improved SOS-based model (henceforth called *Model III*), where the in-phase and quadrature components of the complex envelope of the fading signal

TABLE II
MAXIMUM VALUE OF δ_o

Normalized Doppler frequency, $f_D T_s$	*Max. step size,* δ_o
$f_D T_s \le 0.0001$	0.00000005
$f_D T_s \le 0.0005$	0.0000001
$f_D T_s \le 0.001$	0.0000005
$f_D T_s \le 0.005$	0.000001
$f_D T_s \le 0.01$	0.00001

are written in discrete time as follows:

Model III:

$$c_i[m] = \sqrt{\frac{2}{N}} \sum_{n=1}^{N} \cos\left(2\pi f_D T_s m \cos(\alpha_n[m]) + \varphi_n\right) \quad (2)$$

$$c_q[m] = \sqrt{\frac{2}{N}} \sum_{n=1}^{N} \cos\left(2\pi f_D T_s m \sin(\alpha_n[m]) + \psi_n\right) \quad (3)$$

$$\alpha_n[m] = \frac{2\pi n - \pi + \theta[m]}{4N}, \qquad n = 1, \cdots, N.$$

This model is similar to *Model I* but here θ (and the corresponding angles of arrival α_n) are stationary stochastic processes rather than random variables. This key modification was inspired by the measurements in [37]. We note that in isotropic scattering, $\theta[m]$ is uniformly distributed over $[-\pi, \pi)$ and the angle changes continuously and only very slowly. Thus, $\theta[m]$ should be highly correlated. To generate the slowly changing and highly correlated $\theta[m]$, we propose to use a random walk process [37]. The RWP θ is initialized with a uniformly distributed random value between $[-\pi, \pi]$ and an initial positive direction towards π. The RWP updates towards π with a very small random step size $\delta_o \times u[m]$ in the positive direction, where $u[m]$ is a generated random variable with independent, uniformly-distributed samples over $[0, 1)$. To obtain a slowly changing RWP θ, the coefficient δ_o is chosen to be small enough that the successive random steps $\delta_o \times u[m]$ produce highly correlated angles of arrival. Some suggested predefined values of δ_o, which is a function of the normalized Doppler rate and the precision of the variables used when performing fixed-point simulation, are given in Table II. When the magnitude of the RWP exceeds π, then the update direction is reversed thus causes decreases towards $-\pi$. The update procedure for RWP $\theta[m]$ is presented as Algorithm 1.

It is straightforward to extend the proposed Rayleigh model to support Rician fading channels. We assume that the LOS or specular component is time-varying and stochastic [22]. In our model the LOS component will employ a zero-mean stochastic sinusoid with a fixed angle of arrival, a random initial phase, and a Doppler frequency f_{D_o} [22]. The quadrature components of the resulting Rician model can then be expressed in discrete time as follows:

Model IV:

$$r_i[m] = \frac{1}{\sqrt{K+1}} c_i[m] + \frac{\sqrt{K}}{\sqrt{K+1}} \cos(2\pi f_{D_o} T_s m \cos\theta_o + \phi_o),$$

Algorithm 1 The update procedure for random walk process θ

Initialize $\delta_o = \epsilon \ll 1$, $\theta[0] = U(-\pi, \pi)$;
for $m > 0$ **do**
  $\theta[m] = \theta[m-1] + (\delta_o \times u[m])$;
  if $\theta[m] > +\pi$ **then**
    $\theta[m] = +\pi$; $\delta_o = -\delta_o$;
  end if
  if $\theta[m] < -\pi$ **then**
    $\theta[m] = -\pi$; $\delta_o = -\delta_o$;
  end if
end for

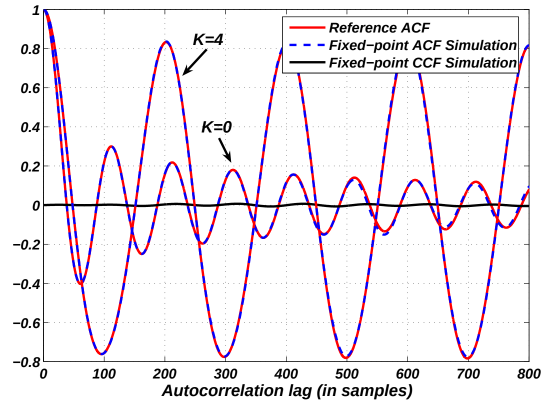

Fig. 5. ACF and CCF of 2×10^6 generated Rayleigh and Rician fading samples with $f_D T_s = 0.01$, $\theta_o = \pi/4$, and $N = 8$.

$$r_q[m] = \frac{1}{\sqrt{K+1}} c_q[m] + \frac{\sqrt{K}}{\sqrt{K+1}} \sin(2\pi f_{D_o} T_s m \cos\theta_o + \phi_o),$$

where the Rician factor K is the ratio of the specular power to the scattered power. θ_o and ϕ_o are the angle of arrival and the initial phase of the LOS component, respectively, which are uniformly distributed random variables over $[-\pi, \pi)$.

Proving the ergodicity of our new model appears to be intractable; nevertheless, numerous bit-true fixed-point simulations have been performed to evaluate the statistical properties of the proposed Rayleigh and Rician fading channels. For example, a block of 2×10^6 fading samples using $N = 8$ sinusoids with $f_D T_s = 0.01$ and $\theta_o = \pi/4$ was generated in one simulation trial and the time-averaged statistical properties of both the Rayleigh and Rician fading processes were measured. Fig. 5 plots the ideal ACF along with the ACF and CCF of the fading samples generated by the new model. As Fig. 5 shows, the generated ACF accurately matches the theoretical ACF. In addition, the generated CCF is very small. Significant improvement in the time-averaged ACF and CCF properties of generated fading samples using *Model III* can be seen by comparing Fig. 5 with the ACF and CCF statistics of *Models I* and *II*, shown in Figs. 3 and 4, respectively. Figures 6 and 7 plot the PDF and the CDF of the generated Rayleigh and Rician fading samples against the reference functions. Again, a close match can be observed between the theoretical functions and the simulated statistics.

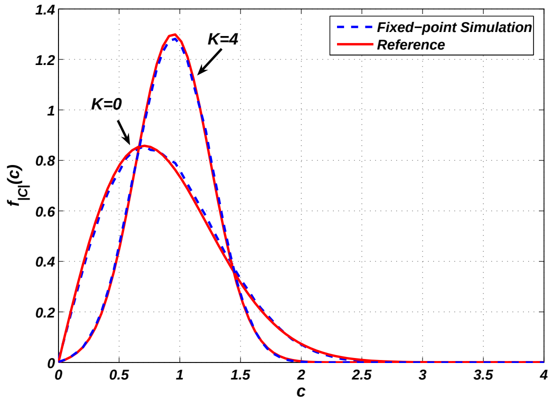

Fig. 6. PDF of 2×10^6 generated Rayleigh and Rician fading samples with $f_D T_s = 0.01$, $\theta_o = \pi/4$, and $N = 8$.

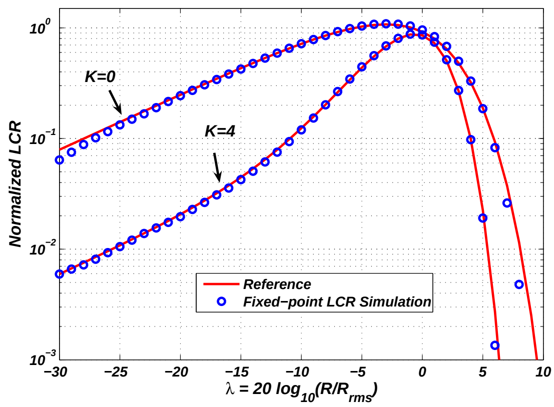

Fig. 8. LCR of 2×10^6 generated Rayleigh and Rician fading samples with $f_D T_s = 0.01$, $\theta_o = \pi/4$, and $N = 8$.

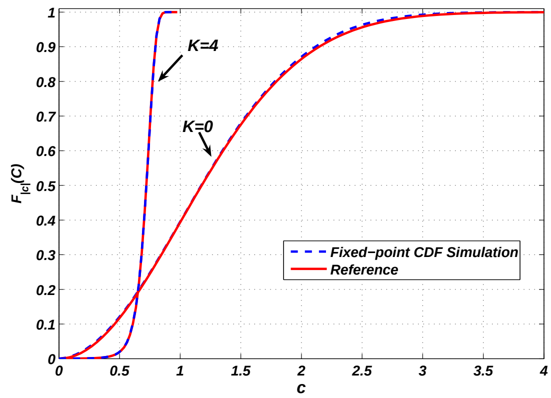

Fig. 7. CDF of 2×10^6 generated Rayleigh and Rician fading samples with $f_D T_s = 0.01$, $\theta_o = \pi/4$, and $N = 8$.

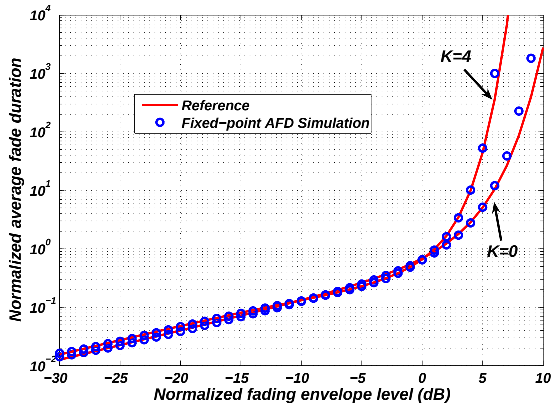

Fig. 9. AFD of 2×10^6 generated Rayleigh and Rician fading samples with $f_D T_s = 0.01$, $\theta_o = \pi/4$, and $N = 8$.

Two other important statistical properties of the generated fading samples are the LCR and the AFD [5]. They characterize important aspects of the temporal behavior of envelope fluctuations. The LCR is the rate at which the envelope crosses a specified level with a positive slope. The AFD indicates how long the envelope stays below a given threshold. Since the AFD determines the average length of burst errors, it has a great impact on the design and testing of wireless communication systems [38], [39]. The LCR and AFD of the envelope of the generated Rayleigh and Rician fading samples and the theoretical functions are plotted in Figs. 8 and 9, respectively. Once again a close match between the generated statistics and the theoretical functions can be observed. Taken together, the simulation results in Figs. 5-9 provide strong empirical evidence that both *Model III* and *Model IV* can faithfully reproduce the properties of Clarke's model.

IV. Implementation of the Fading Channel Simulator

In this section we describe an efficient design that implements the proposed *Model III* on a single FPGA. For a fading channel simulator, one of the important decisions is the choice of the PNG that generates uniformly-distributed unsigned values between $(0, 1)$. Moreover, the fading channel simulator must accurately create very long sequence of fading samples so that the test conditions do not repeat during test runs. This implies that the PNG should have a long repetition period. We used a combined linear PNG that has substantially better randomness properties and a longer period compared to conventional linear PNGs, such as the widely-used linear feedback shift register [40]. The block diagram of the selected 32-bit combined Tausworthe generator with period $\rho \approx 2^{113}$ (`CTG2To113`) [41] is shown in Fig. 10. Note that the registers $s_j, j = 1, \cdots, 4$ store four 32-bit variables that are initialized with four separate seeds. Although the randomness properties of each of the four components is very good, bitwise XORing the output of these four components produces even better randomness properties together with a much longer repetition period.

To calculate the $\sin(\alpha_n[m])$ and $\cos(\alpha_n[m])$ values, first we note that for the n-th sinusoid at time index m we can

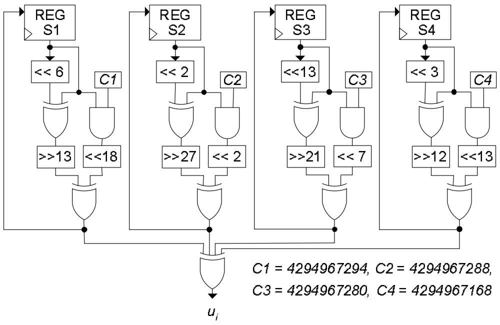

Fig. 10. Logic diagram of a CTG2To113.

calculate $\alpha_n[m]$ using the following iterative equation

$$\begin{aligned}\alpha_n[m] &= \frac{2\pi n - \pi + \theta[m]}{4N} \\ &= \frac{2\pi n - \pi + \theta[m-1]}{4N} + \delta' \\ &= \alpha_n[m-1] + \delta'.\end{aligned}$$

Thus $\cos(\alpha_n[m])$ and $\sin(\alpha_n[m])$ can be approximated as follows:

$$\begin{aligned}\cos(\alpha_n[m]) &\simeq \cos\left(\alpha_n[m-1]\right) - \delta' \sin\left(\alpha_n[m-1]\right), \\ \sin(\alpha_n[m]) &\simeq \sin\left(\alpha_n[m-1]\right) + \delta' \cos\left(\alpha_n[m-1]\right).\end{aligned}$$

The sine and cosine values used to calculate $\sin(\alpha_n[m])$ and $\cos(\alpha_n[m])$, respectively, are stored in four dual-port (for $N = 8$) memories TBLROM12, TBLROM34, TBLROM56, and TBLROM78, each configured in 512×32 format. We use N 60-bit multipliers to multiply the 12-bit $\cos\alpha_n[m]$ value with the 48-bit value of mf_DT_s. Similarly, N 60-bit multipliers are required for the quadrature component. Eight dual-port ROMs store cosine values used to calculate the in-phase and quadrature components, $c_i[m]$ and $c_q[m]$. The hardware-based fading channel simulator design was adjusted carefully to ensure accurate fixed-point representations of the variables while minimizing the computational resources. Specifically, the stochastic process θ was represented in 32-bit format, while $\phi[n]$ and $\psi[n]$ used 10-bit precision. The values of $\sin(\alpha_n[m])$ and $\cos(\alpha_n[m])$ were represented in 12-bit format and the cosine values required to calculate $c_i[m]$ and $c_q[m]$ were represented in 16-bit fixed-point format.

The proposed fading channel *Model III* was implemented as a Verilog hardware description language model and synthesized for three typical FPGA devices. As shown in the third column of Table III, the implementation of the Rayleigh fading channel simulator on a Xilinx Virtex2P XC2VP100-6 FPGA uses 5% of the configurable slices, requires 48 dedicated 18×18 multipliers, and 12 BRAMs. The maximum sampling rate of the fading channel simulator on a Altera Stratix EP1S80F1508C6 FPGA is slower while utilizing only 1% of the configurable logic elements and 128 of the dedicated DSP blocks. To ensure the statistical accuracy of the generated fading samples, the hardware-based channel simulator was designed so that it regenerates the same samples produced by the bit-true software simulator. The proposed design is readily scalable to exploit the available FPGA capacity. As the implementation results in Table III show, a multiple antenna systems with up to 10 channels (as each channel requires 10% of the dedicated multipliers) can be implemented on a single Xilinx Virtex-II Pro XC2VP100-6 FPGA. Fig. 11 shows the layout of a $472,430\ \mu m^2$ semicustom integrated circuit implementation of the Rayleigh fading channel simulator designed in a 90-nm CMOS technology using a dual-threshold standard cell library. The core was targeted to operate at 500 MHz, generating 500 million 16-bit complex fading variables per second.

TABLE III
IMPLEMENTATION OF THE PROPOSED RAYLEIGH FADING CHANNEL SIMULATOR ON THREE DIFFERENT FPGAS

Device family	I[a]	II	III
Max. clock freq. (MHz)	195.61	204.75	103.01
Output rate (MSamps/sec)	195	204	103
Slice utilization	2447 (9%)	2444 (5%)	1292 (1%)
Dedicated resource utilization	48 (9%)	48 (10%)	128 (72%)
Number of BRAMs	12 (3%)	12 (2%)	2%

[a]Design I was synthesized for a Xilinx Virtex4 XC4VSX55-11. Design II was synthesized for a Xilinx Virtex2P XC2VP100-6. Finally, Design III was synthesized for an Altera Stratix EP1S80F1508C6.

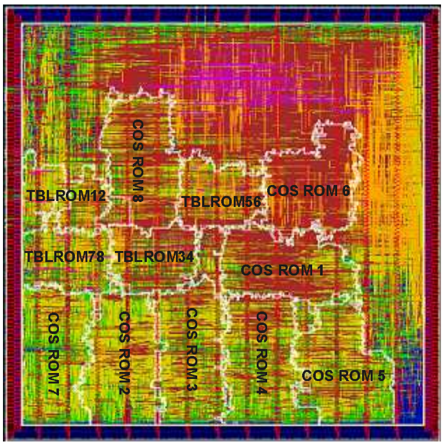

Fig. 11. Layout of the 500 MHz semicustom Rayleigh fading channel simulator.

The reason that the above implementation scheme, which first appeared in an earlier form in [42], uses a relatively large number of dedicated multipliers is because it requires N 60-bit multipliers to multiply the 12-bit $\cos(\alpha_n[m])$ value with the 48-bit value of mf_DT_s. We now propose a more compact design that utilizes a more efficient operation schedule. It first multiplies f_DT_s with the $\cos(\alpha_n[m])$ value (and also with $\sin(\alpha_n[m])$ for the quadrature components), which requires 16-bit multipliers instead of 48-bit multipliers. Then the results are accumulated in order to obtain the value of $m.(f_DT_s\cos\alpha_n[m])$. The implementation of this new scheme on a Xilinx Virtex2P XC2VP100-6 FPGA uses only 965 (2%) of the configurable slices, requires 16 (3%) dedicated 18×18 multipliers, and 12 (2%) BRAMs, while generating 203 million complex-valued Rayleigh fading samples per second. This revised implementation is significantly smaller than the

TABLE IV
IMPLEMENTATION RESULTS OF RAYLEIGH FADING CHANNEL SIMULATORS USING DIFFERENT MODELS ON A XILINX VIRTEX-II PRO XC2VP100-6 FPGA

Design	New Imp.	A [43]	B [44]
Model	*Model III*	*Model I*	*Model I*
Clock freq. (MHz)	203.99	201.69	210.3
Output rate (MSamps/sec)	203	201	210
Configurable slices	965 (2%)	542 (1%)	8814 (19%)
Dedicated resources	16 (3%)	8 (1%)	256(57%)
On-chip memory blocks	12 (2%)	8	–

scheme used in [42] and allows the implementation of MIMO channels with a moderate number of antennas (for example with 32 separate fading channels) on a single FPGA. A fixed-point implementation of the Rician fading channel simulator on the same device uses 1046 (2%) of the configurable slices, requires 20 (4%) of the dedicated on-chip multipliers, and 14 (3%) of the BRAMs, while generating 194 million complex-valued Rician fading samples per second. One can utilize a time-multiplexing approach to share functional units and some storage resources so that more channels can fit onto a single FPGA. For comparison, key implementation results of two stochastic block-based SOS-based simulators are presented in Table IV. It is important to note that even though we were able to implement a smaller design for *Model I* in [43], this earlier model is not able to accurately reproduce the statistical properties of propagation environments for the continuous simulation of time-varying wireless channels.

V. CONCLUSIONS

We proposed a new sum-of-sinusoid model for simulating Rayleigh and Rician fading channels that has significantly improved statistics. The major improvement in the new model is the use of random walk processes to update the angles of arrival of the sinusoid components. The resulting model produces accurate statistics in each simulation run (i.e., for every generated fading block) and does not require computationally-intensive ensemble averaging over multiple runs. In addition, we presented a significantly smaller implementation compared to the previously proposed design from [42], reducing the required configurable slices and dedicated multipliers resources by over 50%. A compact fixed-point implementation of the new Rayleigh fading channel simulator on a Xilinx Virtex2P XC2VP100-6 field-programmable gate array (FPGA) utilizes only 2% of the configurable slices, requires 3% of the dedicated on-chip multipliers, and 2% of the Block RAMs, while generating over 200 million complex-valued Gaussian samples per second. Utilizing an efficient operation scheduling, the number of paths that can be implemented simultaneously on a FPGA is three times more than the best previous implementation. The ability to implement an entire multipath fading channel simulator on a single FPGA should be a significant improvement for the prototyping and verification of frequency-selective channels and multiple-antenna wireless systems, where multiple independent fading paths are required.

REFERENCES

[1] P. Bello, "Characterization of randomly time-variant linear channels," *IEEE Trans. Commun.*, vol. 11, no. 4, pp. 360–393, 1963.

[2] R. N. Kolte, S. C. Kwatra, and G. H. Stevens, "Computer controlled hardware simulation of fading channel models," *Proc. IEEE Intl. Conference on Communications*, 1998, pp. 1646–1650.

[3] W. C. Jakes, *Microwave Mobile Communications*. Piscataway, NJ: Wiley-IEEE Press, 1994.

[4] J. I. Smith, "A computer generated multipath fading simulation for mobile radio," *IEEE Trans. Veh. Technol.*, vol. 24, no. 3, pp. 39–40, August 1975.

[5] G. L. Stüber, *Principles of Mobile Communication*. New York: Kluwer Academic Publishers, 2001.

[6] *Baseband Studio for Fading*, Technical Overview, N5115A, Agilent Technologies Inc., 2005.

[7] *Full Featured Channel Simulator*, Technical Manual, SIMSTAR-1, Ascom, 2002.

[8] *Wireless Channel Emulator*, Technical Document, SR5500, Spirent Communications, 2006.

[9] *Multipath Fading Simulator*, Product Manual, NJZ-1600B, Japan Radio Co., 2005.

[10] M. A. Wickert and J. Papenfuss, "Implementation of a real-time frequency-selective RF channel simulator using a hybrid DSP-FPGA architecture," *IEEE Trans. Microw. Theory Tech.*, vol. 49, no. 8, pp. 1390–1397, 2001.

[11] R. H. Clarke, "A statistical theory of mobile-radio reception," *Bell System Technical Journal*, vol. 47, pp. 957–1000, 1968.

[12] P. Hoeher, "A statistical discrete-time model for the WSSUS multipath channel," *IEEE Trans. Veh. Technol.*, vol. 41, pp. 461–468, 1992.

[13] Y. R. Zheng and C. Xiao, "Improved models for the generation of multiple uncorrelated Rayleigh fading waveforms," *IEEE Commun. Lett.*, vol. 6, pp. 256–258, 2002.

[14] C. S. Patel, G. L. Stüber, and T. G. Pratt, "Comparative analysis of statistical models for the simulation of Rayleigh faded cellular channels," *IEEE Trans. Commun.*, vol. 53, pp. 1017–1026, 2005.

[15] *NoiseCom MP-2500 Multipath Fading Emulator, Technical Manual*, NoiseCom, Paramus, NJ, 1996.

[16] *Baseband Fading Simulator ABFS, Saving costs through baseband simulation*, Data sheet, Rohde & Schwarz, 2004.

[17] A. Alimohammad, S. F. Fard, B. F. Cockburn, and C. Schlegel, "A compact and accurate Gaussian variate generator," *IEEE Trans. Very Large Scale Integr. (VLSI) Syst.*, vol. 16, no. 5, pp. 517–527, 2008.

[18] W. C. Jakes, *Microwave Mobile Communications*. Piscataway, NJ: Wiley-IEEE Press, 1974.

[19] M. Pätzold, *Mobile Fading Channels*. West Sussex, U.K.:Wiley, 2002.

[20] M. Pätzold, U. Killat, F. Laue, and Y. Li, "On the statistical properties of deterministic simulation models for mobile fading channels," *IEEE Trans. Veh. Technol.*, vol. 47, pp. 254–269, 1998.

[21] C. Xiao, Y. R. Zheng, and N. Beaulieu, "Statistical simulation models for Rayleigh and Rician fading," *Proc. IEEE Intl. Conference on Communications*, 2003, pp. 3524–3529.

[22] C. Xiao, Y. R. Zheng, and N. C. Beaulieu, "Novel sum-of-sinusoids simulation models for Rayleigh and Rician fading channels," *IEEE Trans. Wireless Commun.*, vol. 5, no. 12, pp. 3667–3679, 2006.

[23] M. F. Pop and N. C. Beaulieu, "Limitations of sum-of-sinusoids fading channel simulators," *IEEE Trans. Commun.*, vol. 49, pp. 699–708, 2001.

[24] M. Pätzold and B. O. Hogstad, "Classes of sum-of-sinusoids Rayleigh fading channel simulators and their stationary and ergodic properties Part I," *WSEAS Transactions on Mathematics*, vol. 5, no. 2, pp. 222–230, 2006.

[25] P. Dent, G. E. Bottomley, and T. Croft, "Jakes fading model revisited," *Electronics Letters*, vol. 29, no. 13, pp. 1162–1163, June 1993.

[26] Y. Li and X. Huang, "The simulation of independent Rayleigh faders," *IEEE Trans. Commun.*, vol. 50, no. 9, pp. 1503–1514, 2002.

[27] A. Alimohammad and B. F. Cockburn, "Modeling and hardware implementation aspects of fading channel simulators," *IEEE Trans. on Veh. Technol.*, vol. 57, no. 4, pp. 2055–2069, 2008.

[28] E. N. Gilbert, "Energy reception for mobile radio," *Bell System Technical Journal*, pp. 1779–1803, October 1965.

[29] M. Pätzold, R. Garcia, and F. Laue, "Design of high-speed simulation models for mobile fading channels by using table look-up techniques," *IEEE Trans. Veh. Technol.*, vol. 49, no. 4, pp. 1178–1190, July 2000.

[30] Y. R. Zheng and C. Xiao, "Simulation models with correct statistical properties for Rayleigh fading channels," *IEEE Trans. Commun.*, vol. 51, pp. 920–928, 2003.

[31] C. A. G. de Leon, M. C. Bean, and J. S. Garcia, "Generation of correlated Rayleigh-fading envelopes for simulating the variant behavior of indoor radio propagation channels," *Proc. IEEE Veh. Tech. Conf.*, 2004, pp. 4245–4249.

[32] Z. Wu, "Model of independent Rayleigh faders," *Electronics Letters*, vol. 40, no. 15, pp. 949–951, 2004.

[33] A. Papoulis and S. U. Pillai, *Probability, Random Variables and Stochastic Processes*. McGraw-Hill, 2002.

[34] C.-H. Liao, T.-P. Wang, , and T.-D. Chiueh, "A novel low-complexity Rayleigh fader for real-time channel modeling," *IEEE ISCAS*, 2007, pp. 2602–2605.

[35] P. Hoeher and A. Steingaß, "Modeling and emulation of multipath fading channels using controlled randomness," *Proceedings ITG-Fachtagung "Wellenausbreitung bei Funksystemen und Mikrowellensystemen"*, 1998, pp. 209–220.

[36] A. Zajić and G. L. Stüber, "Efficient simulation of Rayleigh fading with enhanced de-correlation properties," *IEEE Trans. Wireless Commun.*, vol. 5, no. 7, pp. 1866–1875, 2006.

[37] P. Pampaloni and S. Paloscia, *Microwave Radiometry and Remote Sensing of the Earth's Surface and Atmosphere*. VNU Science Press, 2000.

[38] K. Ohtani, K. Daikoku, and H. Omori, "Burst error performance encountered in digital land mobile radio channel," *IEEE Trans. on Veh. Technol.*, vol. 30, no. 4, pp. 156–160, 1981.

[39] J. M. Morris, "Burst error statistics of simulated Viterbi decoded BPSK on fading and scintillating channels," *IEEE Trans. Commun.*, vol. 40, pp. 34–41, 1992.

[40] P. L'Ecuyer, "Tables of maximally equidistributed combined LFSR generators," *Math. of Comp.*, vol. 68, no. 225, pp. 261–269, 1999.

[41] ——, "Maximally equidistributed combined Tausworthe generators," *Math. of Comp.*, vol. 65, no. 213, pp. 203–213, 1996.

[42] A. Alimohammad, S. F. Fard, B. F. Cockburn, and C. Schlegel, "An improved SOS-based fading channel emulator," *IEEE Fall Veh. Tech. Conf.*, 2007, pp. 931–935.

[43] A. Alimohammad and B. F. Cockburn, "Compact implementation of a sum-of-sinusoids Rayleigh fading channel simulator," *Proc. IEEE ISSPIT*, 2006, pp. 253–257.

[44] ——, "A reconfigurable SOS-based Rayleigh fading channel simulator," *IEEE Intl. Workshop on Signal Processing Systems, Design and Implementation*, 2006, pp. 39–44.